Instrumentation, Nondestructive Testing, and Finite-Element Model Updating for Bridge Evaluation Using Strain Measurements

Masoud Sanayei, M.ASCE[1]; John E. Phelps, M.ASCE[2]; Jesse D. Sipple, M.ASCE[3]; Erin S. Bell, M.ASCE[4]; and Brian R. Brenner, M.ASCE[5]

Downloaded from ascelibrary.org by Tufts University on 06/08/15. Copyright ASCE. For personal use only; all rights reserved.

Abstract: A baseline finite element model was developed for bridge management and calibration using nondestructive test data. The model calibration technique was evaluated on the Vernon Avenue Bridge over the Ware River in Barre, Massachusetts. This newly constructed bridge was instrumented throughout its construction phases in preparation for a static truck load test performed before the bridge opening. The strain data collected during the load test was used to calibrate a detailed baseline finite element model in an effort to represent the 3D system behavior of the bridge. Three methods of load ratings were used and compared: (1) conventional method, (2) conventional method updated by using NDT data, and (3) finite element model calibrated with NDT data. **DOI: 10.1061/(ASCE)BE.1943-5592.0000228.** *© 2012 American Society of Civil Engineers.*

CE Database subject headings: Bridges; Superstructures; Full-scale tests; Field tests; Nondestructive tests; Strain; Measurement; Finite element method; Load tests; Structural health monitoring.

Author keywords: Bridge; Superstructure; Full scale; Field testing; Strain measurements; Finite elements; Model calibration; Load testing; Load rating; Structural health monitoring; SHM.

Introduction

According to the Federal Highway Administration, traffic volumes in the US have nearly doubled since 1984, from 1.65 trillion total miles traveled annually to nearly three trillion miles in 2009 (FHWA 2009). As traffic continues to increase, the number of highway bridges in need of major rehabilitation or replacement has also increased. Recent events such as the I-35W bridge collapse in Minnesota and the unexpected closings of the Oakland Bay Bridge in California have helped to illustrate the severity of the conditions of this nation's bridges. In response to this challenge of aging infrastructure, researchers across industries have investigated structural health monitoring approaches that can help address the complex safety, reliability, and economic issues associated with the long-term aspects of bridge safety and maintenance.

With advances in finite element software, instrumentation, and data management, it is now feasible to create detailed 3D finite element models (FEMs) of highway bridges and calibrate the FEMs using collected field data. These calibrated baseline FEMs can be prepared to document the design decisions made by engineers and also assist bridge owners in all future bridge management decisions. For the purpose of this discussion, a baseline model is defined as a detailed 3D FEM that has been calibrated, through a load test, therefore capturing the behavior of the as-built bridge. In essence, a baseline model is an analytical physics-based representation of the structure that reflects the actual response of the bridge under a defined loading. In comparison to baseline models, traditional "design" models are not intended to be realistic representations of actual structural response. They consider individual structural components instead of overall structural system behavior, and the design is enveloped to address the greatest possible demand for each individual component. This approach is appropriately conservative, in part, because it is not possible for each individual component to experience maximum demand simultaneously.

A baseline model holds great potential in assisting bridge owners because it may be used to evaluate long-term bridge performance. The eventual goal is development of an electronic Structural Health Monitoring (SHM) System that is complementary to visual inspections. This SHM System could be used to compare predicted and measured response and provide the owner with continuous information about overall bridge performance over time. The baseline model could also be updated to account for deterioration and used for subsequent analysis and load ratings. Development of a 3D FEM and instrumentation plan in the initial design process provides a tool for improved long-term structural evaluation and overall bridge management. The 3D FEM should be calibrated using measured bridge response. Transformation from a 3D FEM to a baseline model is achieved by an initial load test

[1]Professor, Dept. of Civil & Environmental Engineering, Tufts Univ., Medford, MA 02155 (corresponding author). E-mail: masoud.sanayei@tufts.edu

[2]Assistant Structural Engineer, Gill Engineering Associates, Inc., Needham, MA 02494; formerly, Graduate Student, Tufts Univ., Medford, MA 02155. E-mail: jphelps@gill-eng.com

[3]Doctoral Candidate, Dept. of Civil & Environmental Engineering, Tufts Univ., Medford, MA 02155. E-mail: jesse.sipple@tufts.edu

[4]Associate Professor, Dept. of Civil Engineering, Univ. of New Hampshire, Durham, NH 03824. E-mail: erin.bell@unh.edu

[5]Professor of Practice, Dept. of Civil & Environmental Engineering, Tufts Univ., Medford, MA 02155; Vice President, Fay Spofford & Thorndike, Burlington, MA 01803. E-mail: brian.brenner@tufts.edu

Note. This manuscript was submitted on June 11, 2010; approved on February 3, 2011; published online on December 15, 2011. Discussion period open until June 1, 2012; separate discussions must be submitted for individual papers. This paper is part of the ***Journal of Bridge Engineering***, Vol. 17, No. 1, January 1, 2012. ©ASCE, ISSN 1084-0702/2012/1-130–138/$25.00.

and can be continued throughout the life of the bridge as a new portion of scheduled maintenance programs.

An extensive review of SHM methods can be found in Doebling et al. (1996) and Sohn et al. (2003). Chung and Sotelino (2006) investigated a number of different FEM techniques for modeling composite girder bridges. They found good agreement between the FEM and the full-scale laboratory bridge test when midspan strains were compared. FEM mesh size has been a topic of investigation for SHM. Zhang and Aktan (1997) discussed two different levels of FEM for use in bridge evaluation and concluded that a simple 2D model had potential because of its relative accuracy when compared to the measured data. Mabsout et al. (1997) investigated four different FEMs and found that the FEMs reported lower live load distribution factors than AASHTO's standard and LRFD specifications (AASHTO 2002; AASHTO 2010b).

Cardini and DeWolf (2008) presented an approach for using strain data from a multigirder composite steel bridge to analyze live load distribution factors, peak strain values, and neutral axis locations for a long-term SHM system. Alampalli and Lund (2006) presented a case study where measured strain data were used to predict the remaining fatigue life of certain bridge components. Barr et al. (2006) used a FEM that was verified by NDT data to calculate more refined load rating factors leading to an eventual increase in load rating for a three-span highway bridge. Chajes and Shenton (2005) present a method for load rating on the basis of the NDT data that includes the investigation of lateral load distribution, support fixity, composite action, and the effect of secondary members. Jauregui and Barr (2004) used collected data to verify a FEM that was used to refine the original load rating for a precast, prestressed concrete girder bridge. These works were used to refine the instrumentation, modeling, and data postprocessing procedures used in this article.

This article discusses an approach for implementing an instrumentation system during bridge construction, performing a nondestructive load test before the bridge opening, creating a detailed 3D FEM, calibrating the model using the collected measured strains, and finally, bridge load rating evaluation. The approach was applied to the design and construction of Vernon Avenue over the Ware River in Barre, Massachusetts. The 3D FEM was created before construction on the basis of design drawings and in consultation with bridge designers. Calibration of the 3D FEM was performed using the load test data resulting in the baseline model. A comparison was made between the load rating factors on the basis of AASHTO and the rating factors calculated using the baseline model and the load test data.

This research was performed as part of a National Science Foundation Partnership for Innovation Project entitled, "Whatever Happened to Long-Term Bridge Design?" Project goals include development of a baseline model and protocols for consideration of long-term bridge issues as part of the initial design process. The project's title is inspired by the paper written by Thomas Kuesel (1990), "Whatever Happened to Long-Term Bridge Design?"

Vernon Avenue Bridge

Vernon Avenue Bridge over the Ware River was constructed during the summer of 2009 by ET&L Corporation and opened in September 2009 (Fig. 1). The bridge was designed according to Massachusetts Department of Transportation (MassDOT) specifications by Fay, Spofford, & Thorndike. The bridge is owned by the town of Barre. It is a continuous three-span concrete slab on steel stringer bridge. Spans one and three are 11.75 m (38.55 ft) in length, whereas the middle span is 23.5 m (77.1 ft). The bridge structure consists of a 200 mm (7.87 in.) thick concrete deck composite with six steel girders. Two outrigger beams are present at the north end of span 3 to support an increase in deck width as Vernon Avenue connects to Route 122. A section view of the bridge is shown in Fig. 2.

Fig. 1. Completed Vernon Ave. bridge, September 2009

Instrumentation

Instrumentation began in June 2009 and was completed in October 2009. Many different types of sensors were installed, including 100 strain gauges, 16 biaxial-tiltmeters, 16 accelerometers, 30 concrete temperature sensors, 36 girder temperature sensors, and two pressure plates. All instrumentation installed on the bridge is environmentally protected. After more than one year of in-service use, there have not been any signs of instrumentation failures or decrease in the level of service of the monitoring system. Sensor and data acquisition performance and reliability will be monitored over time and documented.

This article discusses the use of measured static strains. Instrumentation was installed at 13 stations along the length of the bridge (Fig. 3). Strain gauges were installed on all six girders at stations two, four, six, eight, and ten. Each interior girder was instrumented with four gauges at each station, including two on the top side of the bottom flange with one on each side of the web, and two on the bottom side of the top flange with one on each side of the web. Each strain gauge was installed approximately 75 mm (3 in.) from the outer edge of the flange on which it is attached. This is halfway between the edge of the flange and face of the web. The exterior girders were instrumented with strain gauges only located on the interior side of the web to reduce exposure to the elements and lessen the visual effect of the instrumentation.

All strain gauge wires were run along the length of the bridge to the south abutment where they were connected to iSite data acquisition boxes provided by Geocomp Corporation. The iSite boxes were attached to the bottom flange of the steel girders (Fig. 4). All iSite boxes were then connected using Ethernet cables to a central hub located in a box between girders three and four. The data acquisition system can be remotely accessed through the internet by an IP phone on-site. This arrangement allows for collected data temporarily stored in each iSite box to be downloaded and saved to iSite Central located at Geocomp's facilities. The stored data at iSite Central can be viewed and downloaded through the Internet by authorized users.

J. Bridge Eng. 2012.17:130-138.

Downloaded from ascelibrary.org by Tufts University on 06/08/15. Copyright ASCE. For personal use only; all rights reserved.

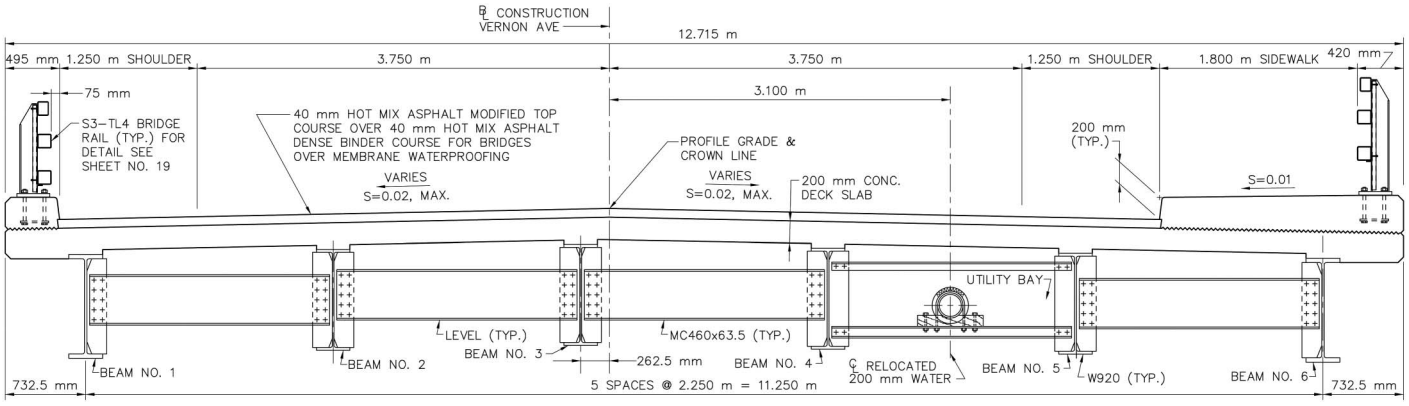

Fig. 2. Vernon Avenue section view (used with permission from FST Inc.)

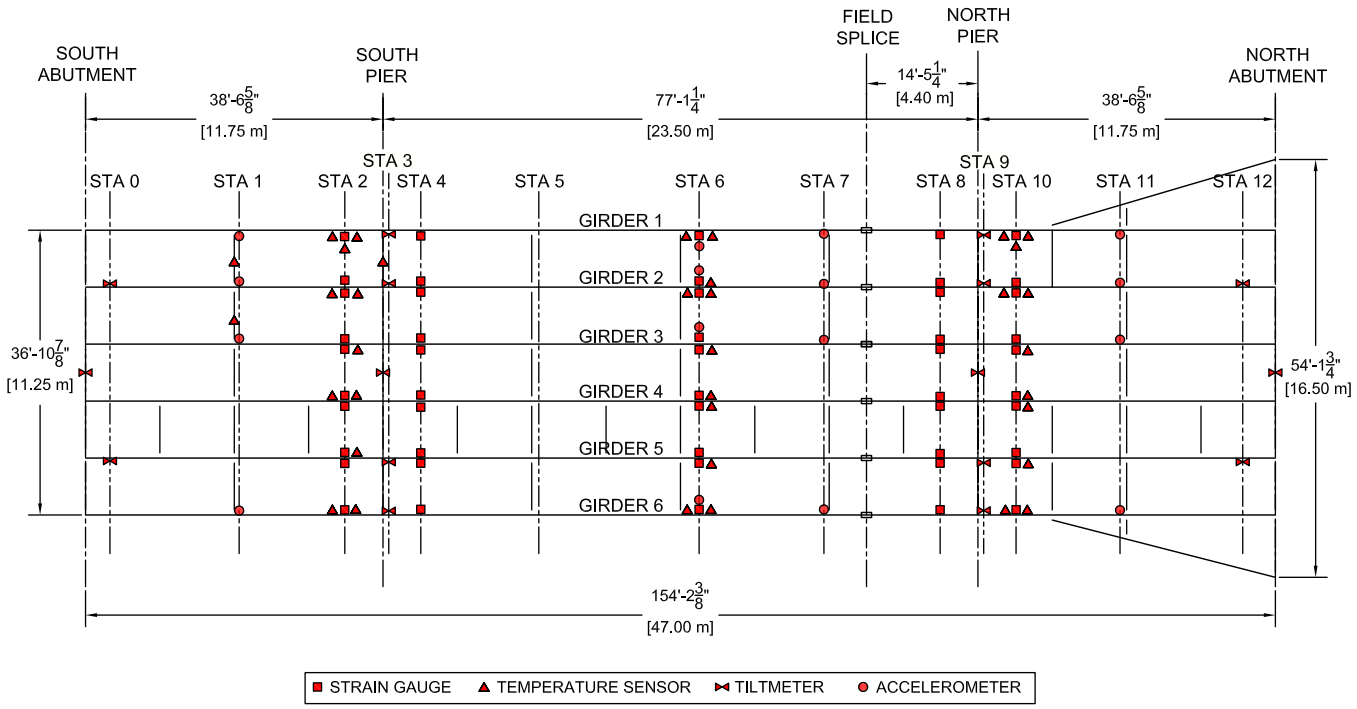

Fig. 3. Vernon Avenue instrumentation plan

Nondestructive Load Test

A static load test was performed before the bridge opening. For this test, strain readings were sampled at 200 Hz. The goal of the static load test was to capture the response of the bridge as a test truck traveled across. The load test responses were then replicated using the FEM, and the results were compared to the collected data.

In preparation for the load test, three travel lanes were defined along the length of the bridge from south to north. Travel lanes X1 and X3 were 0.61 m (2 ft) off of the west curb and 0.76 m (2.5 ft) off of the east curb, respectively. Travel lane X2 was located directly in the center roadway. The truck used for the load test was a triaxle dump truck. Each wheel was weighed using individual scales (Fig. 5). The wheels were weighed three times before the test, and again three times after the test to account for any weight shift. The average axle weights were calculated to be 87 kN (19.63 kips), 119 kN (26.62 kips), and 118 kN (26.54 kips) for the first, second, and third axles, respectively. The wheels on each

Fig. 4. On-site data acquisition system

J. Bridge Eng. 2012.17:130-138.

Downloaded from ascelibrary.org by Tufts University on 06/08/15. Copyright ASCE. For personal use only; all rights reserved.

Fig. 5. Load test truck

axle were spaced at 2.13 m (7.00 ft) and 1.65 m (6.08 ft) for the front and back axles. The front axle was spaced 5.05 m (16.58 ft) from the front rear axle, and the two rear axles were spaced 1.43 m (4.67 ft).

During the load test, two types of tests were performed. The first test was a crawl speed test where the truck moved along the three paths at approximately 0.50 m per (1.10 mph). For this test, the truck traveled at a slow speed to minimize any dynamic effects that could affect the data. The second test featured a series of loadings with the truck stopped at a location. For this series of tests, the truck traveled along the bridge and stopped at each designated stop location for approximately 10 s. A total of nine runs were performed, three runs for each travel lane. Typical measured strain readings for positive moment at the center span and negative moment near the north piers for the crawl speed load test on travel lane X1 are shown in Fig. 6. The location of the strain gauges is shown with the arrow on the bridge graphic. For these figures, and all strain graphs that follow, the four vertical lines represent the four support locations. From the left, the first, second, and third lines represent when the front axle of the truck was located at the south abutment, south pier, and north pier locations respectively. The fourth line represents when the trucks back axle was completely past the north abutment.

Baseline Finite Element Mode

A baseline FEM was created using SAP2000 (Computers and Structures 2010). SAP2000 is backward compatible with computer-aided drawing software packages which will allow for translation of the model into other software packages that may be developed during the service life of the bridge. The initial model consisted of shell elements for the steel girders and diaphragms, and solid elements for the concrete deck and haunch. The decision for using these element types was on the basis of an initial study that examined a number of different modeling procedures used in previous research. The study involved comparing critical midspan values for stress and deflection validations and also taking into account computing time. The FEM used for the initial comparison with the measured strain data was created on the basis of the design drawings. Initially, only the concrete deck, haunch, steel girders, and diaphragms were modeled (Fig. 7).

Support conditions were modeled using spring elements to represent the stiffness of the elastomeric bearing pads. The bearing pad stiffnesses were calculated by using the method outlined in the National Cooperative Highway Research Program Report entitled, "Rotation Limits for Elastomeric Bearings." (Stanton et al. 2008). Additionally, an equation for shear stiffness was derived using the strain displacement relationship of the bearing pad. Details with respect to the calculation of the stiffness values used in the baseline FEM are contained in Phelps (2010).

Manual Model Updating

A critical step in model calibration, whether it be manual tuning or using optimization techniques, is defining an error function to assess the quality of the match between the analytical and measured data. Sanayei et al. (1991) and Sanayei et al. (1992) developed static stiffness-based and static flexibility-based error functions using the residual forces and residual displacements at subsets of degrees of freedom. They used a quadratic scalar objective function for FEM updating, using optimization. Sanayei and Saletnik (1996) extended these methods for using strain measurements for FEM calibration. Sanayei and Imbaro (1997) applied these methods to a laboratory 2-story steel frame subjected to static loads and successfully updated section properties at the component level.

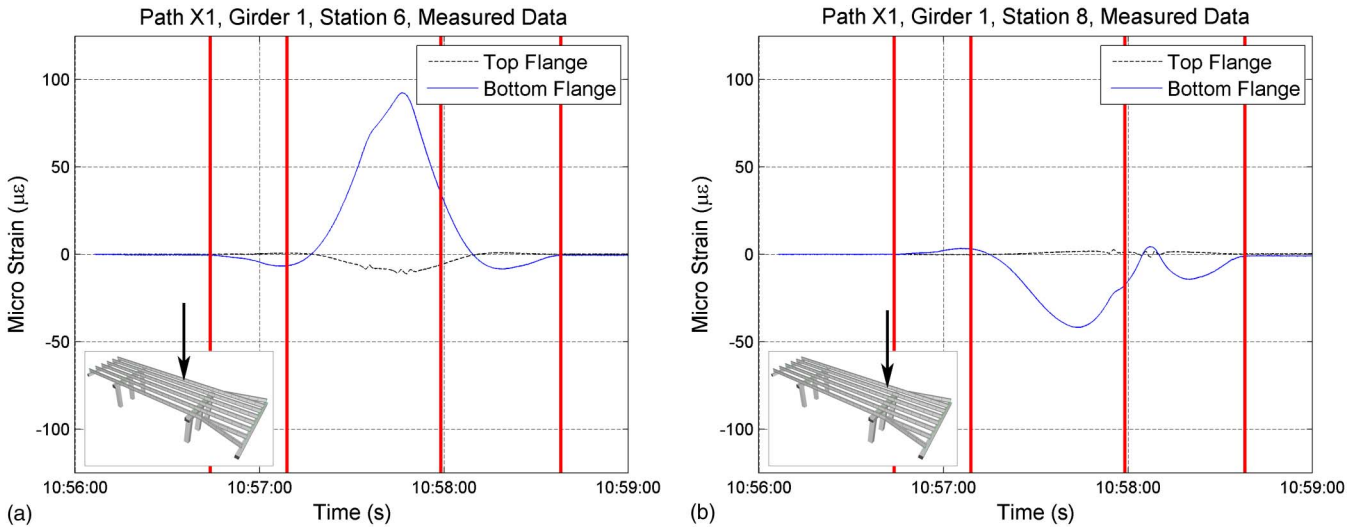

Fig. 6. Measured strains—crawl speed load test: (a) M^+, Girder 1, Station 6; (b) M^-, Girder 1, Station 8

J. Bridge Eng. 2012.17:130-138.

Downloaded from ascelibrary.org by Tufts University on 06/08/15. Copyright ASCE. For personal use only; all rights reserved.

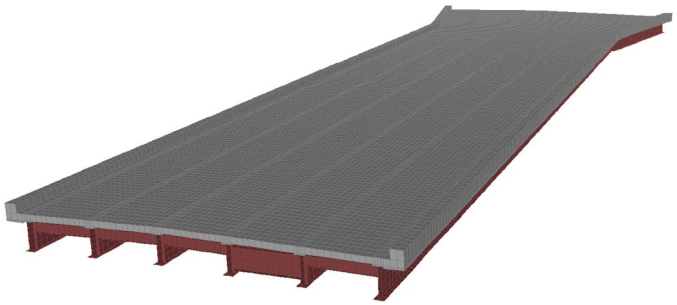

Fig. 7. Initial FEM of the Vernon Ave. bridge

Similar quadratic scalar objective functions were defined by Schlune et al. (2009) and used in conjunction with engineering judgment for manual model updating. One of the objective functions used by Schlune was adapted to be used for this research as follows:

$$J = \frac{1}{n}\frac{1}{s}\sum_{j=1}^{n}\sum_{i=1}^{s}\left(\frac{\varepsilon_{xx}^{a} - \varepsilon_{xx}^{m}}{S^{m}}\right)^{2} \quad (1)$$

where s = total number of strain measurements used for both the measured and experimental strains; and n corresponds to the number of load paths used. The superscripts a and m correspond to the analytical and measured data, respectively. J represents a scalar objective function that is quadratic and weighted by the inverse of the square of the standard deviation of the measured data. It is averaged on the basis of the number of operational sensors and the number of load paths and is unitless. J is used as a guide for assessing the affects of the manual model refinements included in the following sections.

The initial model will have the largest value of J, and as updates are performed, the objective function value should continue to decrease. J is not expected to go to zero in presence of modeling and measurement errors. Note that the absolute value of the error function, J, is not significant. Relative values of J for different models and data sets may be used for comparison of goodness of fit. Also, it should be pointed out that the scalar objective function is not necessarily the only way to quantify the match between the analytical model and measured data. In fact, using this objective function as a means of validating the model using a least square fit approach can hide some differences between the analytical model and measured data. In this discussion, the objective function value for FEM updating is utilized as a recommendation that is guided by engineering judgment.

The initial model used for comparison with the load test data included only the concrete deck, haunch, steel girders, and diaphragms. The initial strain comparison for the crawl speed tests showed that the initial modeled strains matched the measured strain readings relatively well. The overall trend was that the model predicted slightly higher strains than the measured data. The difference between the measured and modeled strains was more evident for the exterior than interior girders. Fig. 8 shows the scalar objective function values for each model refinement made for the crawl speed load test. These FEM refinements always were additive, including previous refinements in the next one. Although the value of the objective function can hide a lot of details in matching the model with the data, it is expected that as major refinements are made to the model, this value will decrease as the overall match between measured and modeled data improves.

The first model refinement performed was the modification of the concrete strength included in the model for the concrete deck and haunch. The initial model used a concrete strength of 30 MPa (4,351 psi) on the basis of the design strength. A modified value of 34.1 MPa (4,946 psi) was used in the updated model on the basis of the average cylinder break test results provided by the MassDOT for the 28 day strength of the concrete. By using the higher strength concrete in the FEM, the modeled strains slightly decreased and, thus, there was a better match with the measured data. The scalar objective function values for the model with the updated concrete strength were slightly lower than the previous initial model, as shown in Fig. 8.

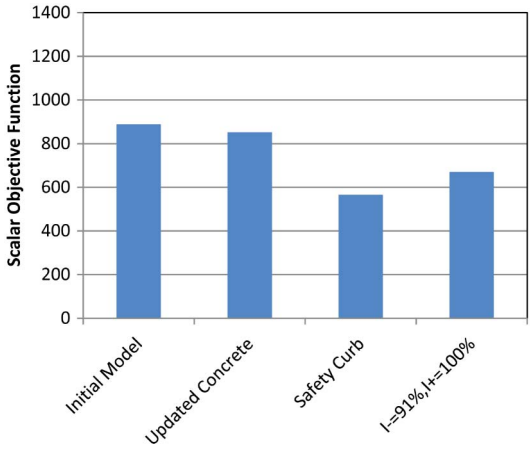

Fig. 8. Scalar objective function—crawl speed test

The second VAB FEM refinement was modeling the safety curbs located on both edges of the bridge deck. Fig. 9 shows that there is reinforcement along the entire bridge length that ensures the safety curbs act compositely with the deck slab. As expected, once the safety curb was modeled, the modeled strains on the exterior girders decreased and approached the measured data. Because the safety curbs are closest to the exterior girders of the bridge, the interior girder strains did not change significantly. The scalar objective function again decreased, suggesting that addressing stiffness of the safety curbs increases the accuracy of the model. The decrease in the scalar objective function was rather significant as shown in Fig. 8.

The final model refinement was the adjustment of the concrete properties to represent the behavior of the reinforced concrete composite deck. Accurately modeling the behavior of the concrete

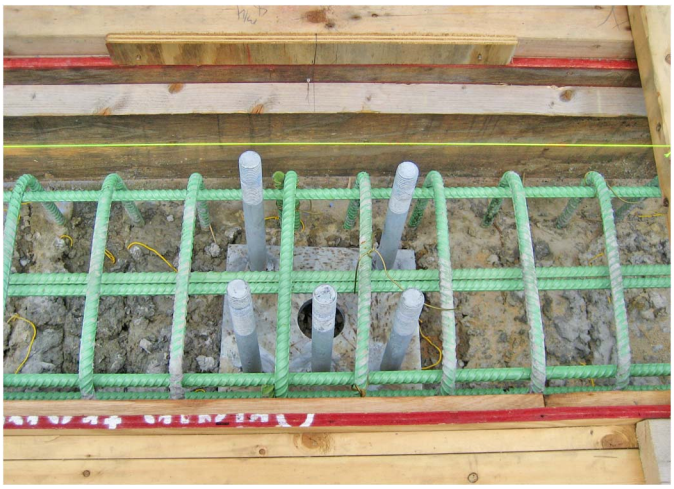

Fig. 9. Safety curb reinforcement

J. Bridge Eng. 2012.17:130-138.

Downloaded from ascelibrary.org by Tufts University on 06/08/15. Copyright ASCE. For personal use only; all rights reserved.

deck was complicated because the bridge is a three-span continuous bridge. Depending on the location of the live load, certain sections of the slab may be in tension. At higher loads, this would cause the concrete to experience minor surface cracks, as per standard concrete behavior, so that tension attributable to negative bending may be transferred to the steel reinforcement. The cracking leads to a reduction in equivalent deck stiffness.

The traditional design approach to address concrete member stiffness is to use the gross moment of inertia. The American Concrete Institute (ACI) provides an approximate procedure for calculating the "effective" moment of inertia after surface cracking has initiated. Although concrete tensile strength is not relied upon at all in design, for calculation of cracking, a tensile capacity up to the modulus of rupture is assumed to be present. Under negative bending, when this capacity is reached, the concrete is expected to crack and transfer tensile loads to steel reinforcement. The ACI method of effective moment of inertia provides an approximate approach for calculating the stiffness reduction. It is suitable and conservative for design, but it is not sufficiently accurate for baseline modeling, which seeks to capture the actual bridge structural response.

In fact, no simple way exists of precisely modeling concrete cracking and stiffness reduction under tension. This is because concrete cracking, when it is initiated, is highly nonlinear and the structure experiences an almost unlimited number of stiffness conditions as the deck cracks, loads are redistributed, and surface cracking continues.

To account for this behavior, the baseline model was manually updated by reducing values of EI in the negative moment region of the deck. With respect to FE modeling, although adjusting the moment of inertia of the composite concrete deck and steel girders in the FEM is complex, the value for the modulus of elasticity of the concrete, E_c, can be more easily modified leading to the same result. As a result, the final model refinement was the investigation of the overall section stiffness by varying the modulus of elasticity of the concrete in the negative moment zones over the piers.

By modifying the cross-sectional properties of the bridge, the neutral axis locations in the steel girders are also effected. As a result, the neutral axis (NA) of each girder was calculated by using the strain measurements at the top and bottom flanges by using the plane section theory. The concrete properties were adjusted until there was good correlation between the NA's calculated from the measured and analytical data. After investigating the neutral axis plots of the measured data, it was determined that reducing the moment of inertia was necessary only for the areas of the bridge that were in negative bending. As a result of the negative region changing with the location of the live load, a value equal to 20% of each span was assumed to typically be in negative bending (10% at each end). By using this approximate value, E_c was then decreased only in these regions and the neutral axis was plotted and the corresponding scalar objective function value was calculated. This was done until there was a good correlation between the neutral axis location of the FEM and the measured data (Fig. 10).

In Fig. 10, the upper dash-dot horizontal line represents the neutral axis location for the full composite section, including the steel reinforcement. The lower dash-dot horizontal line represents the neutral axis location for the section assuming the concrete is fully cracked. The two vertical red lines represent the pier locations. For positive moment regions using strain gauges at the midspan (Station-6), the actual neutral axis location should be close to the full composite section neutral axis. For sections that are in negative bending regions and close to the north pier (Station-8), it is expected that the neutral axis would be below the full composite section because some concrete cracking has occurred.

Low strain readings present challenges for calculating the location of the neutral axis from both measured data and modeled data. With numerically smaller strains, the calculated location of neutral axis can be easily distorted by measurement noise, and the shape of the strain diagram can be significantly affected by small axial forces. However, when these strain readings are higher, a much smaller change occurs in the strain diagram shape attributable to the aforementioned influences. Thus, the neutral axis calculation becomes stable. As a final filter, only measurements that were greater than 20 micro strains were used for the final neutral axis location comparisons shown in Fig. 10.

On the basis of the neutral axis location graphs, the final effective value used for E_c in the negative regions was 18.0 MPa (2,611 psi). This value for E_c corresponds to a moment of inertia equal to 91% of the previous case. In the negative bending regions of the model, the modeled concrete has a moment of inertia equal to

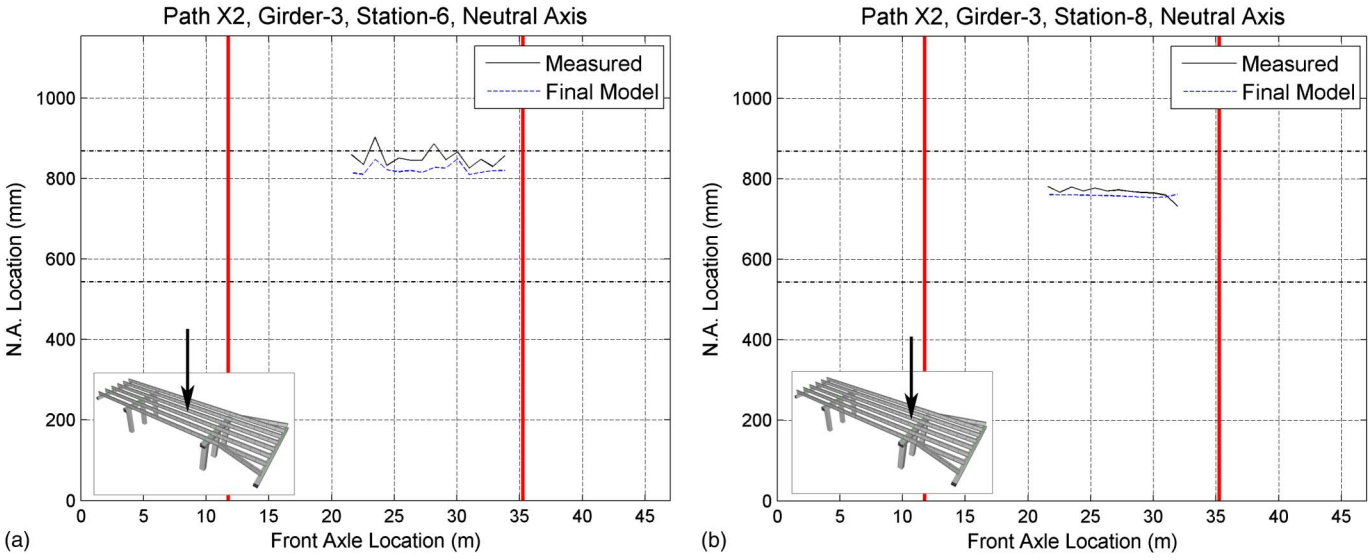

Fig. 10. Neutral axis locations, modeled and measured, crawl speed load test: (a) M^+, Girder 3, Station 6, bottom flange; (b) M^-, Girder 3, Station 8, top flange

J. Bridge Eng. 2012.17:130-138.

Downloaded from ascelibrary.org by Tufts University on 06/08/15. Copyright ASCE. For personal use only; all rights reserved.

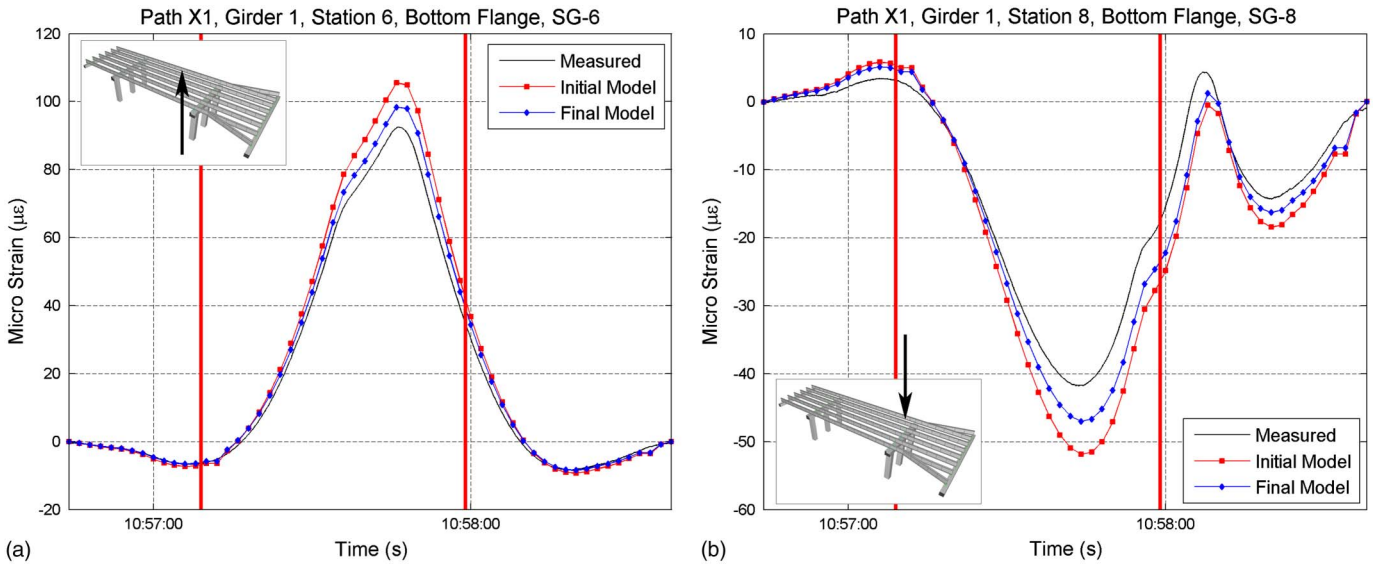

Fig. 11. Modeled and measured strains—crawl speed load test: (a) M^+, Girder 1, Station 6, bottom flange; (b) M^+, Girder 1, Station 8, bottom flange

91% of the modeled concrete in the positive regions. Updating the model in this way showed no significant changes in the strain comparison between the modeled and measured strains. The overall trend actually showed a slight increase in the objective function value for this model (see Fig. 8). If the final model was to be based solely on the scalar objective function, the model with the updated concrete and safety curbs would be used. However, as stated previously, results should always be reviewed with engineering judgment. This is particularly true for smaller changes in the J values which may be overshadowed by modeling errors and measurement errors. When the FEM was modified to take into account the cracking in the negative regions, the analytical neutral axis location in the FEM showed a closer match with the measured location of the NA. For this reason, the final baseline model included the modification of the concrete section properties in the negative moment regions.

Graphs showing the initial and final model strain comparisons for the crawl speed load tests are shown in Fig. 11. The final model shows a significantly better match with the measured values than the initial model. Fig. 11(a) shows the strain for positive moment for the center span (Station-6) and Fig. 11(b) shows the strain for negative moment near the north pier (Station-8).

Load Rating

Bridge owners perform load ratings to analyze and report on bridge capacity over the design life of the structure. Because of deterioration, load ratings may report lower capacity than was provided by the original design. As a result, a bridge may require signage postings to limit allowable truck loads. Load ratings using baseline FEMs may significantly reduce the amount of subjectivity present in conventional load ratings (Yost et al. 2005).

For the Vernon Avenue Bridge, three separate load ratings were calculated. The first was conventional load rating and it was calculated by using Allowable Stress Design (ASD) method in accordance with Standard Specifications for Highway Bridges (AASHTO 2002) and Massachusetts Highway Department Bridge Manual (MassDOT 2005) procedures by using Virtis. The second load rating was calculated by using the measured strain data and Virtis on the basis of the procedure outlined in the AASHTO Manual for Bridge Evaluation (AASHTO 2010a) for load ratings by using diagnostic load tests. The bridge 3D finite element model was then calibrated by using the NDT data. The third load rating was performed by using the calibrated baseline FEM with one load path per girder.

The conventional load rating equation as given by AASHTO is as follows (AASHTO 2010a):

$$\mathrm{RF}_C = \frac{C - A_1 D}{A_2 L(1+I)} \tag{2}$$

where RF_C = rating factor for the live load carrying capacity; C is the capacity of member to resist applied load effects; D is the dead load effect; L is the live load effect; I is the AASHTO Impact factor; and A_1 and A_2 are the dead and live load factors, respectively. For the ASD method, the load factors to be applied to the dead and live loads are 1.0. The conventional load rating for the Vernon Avenue Bridge was performed by using the computer program Virtis5.6. Virtis is a program developed by AASHTOWare that allows the user to input bridge geometry, material properties, cross section properties, and loading conditions for each structural member. The conventional load rating process does not involve use of a 3D system structural model. Typically, load ratings are performed by analysis by using a simplified elemental or grid model of the structure. Performing a load rating by using simplified grid models introduces numerous approximations and assumptions regarding the 3D behavior of the bridge, in particular, how the live loads are distributed to individual girders.

For the load rating using the NDT data, the procedure as outlined in Chapter 8 of the Manual for Bridge Evaluation (AASHTO 2010a) was used. The procedure calculates an adjustment factor that can be multiplied by the conventional load rating factor as:

$$\mathrm{RF}_T = \mathrm{RF}_C K \tag{3}$$

where RF_T represents the rating factor resulting from the diagnostic load test. The adjustment factor K is founded on the benefit derived from the load test and the engineers understanding of the load test. K is equal to one if the load test results agree completely with theory. If K is greater than one, the response of the bridge is more favorable than what the conventional load rating calculated. Similarly, if K is less than one, the response of the bridge is worse than the conventional load rating calculated.

J. Bridge Eng. 2012.17:130-138.

Downloaded from ascelibrary.org by Tufts University on 06/08/15. Copyright ASCE. For personal use only; all rights reserved.

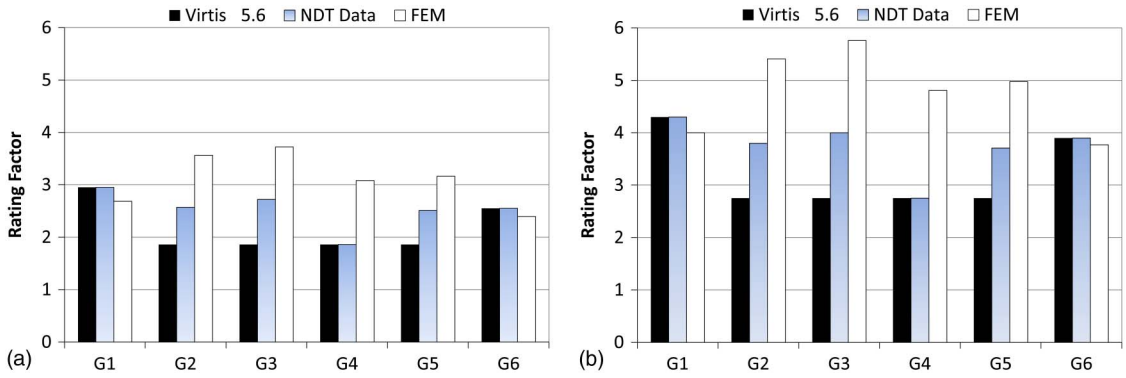

Fig. 12. Vernon Avenue bridge rating factors: (a) inventory; (b) operating

The third load rating for the Vernon Avenue Bridge was calculated using the detailed FEM. To perform the load rating by using the FEM, Eq. (2) was modified to allow the use of manually output maximum longitudinal stresses from SAP2000 as shown in Eq. (4).

In Eq. (4):

$$\mathrm{RF} = \frac{\sigma_{xx}^{C} - \sigma_{xx}^{\mathrm{DL}} - \sigma_{xx}^{\mathrm{SDL}}}{\sigma_{xx}^{\mathrm{LL}}(1+I)} \tag{4}$$

In Eq. (4), σ_{xx}^{C} represents the longitudinal stress capacity of the individual beam under evaluation. The maximum longitudinal stresses resulting from the noncomposite dead loads (DL) and superimposed dead loads (SDL) are subtracted from this stress capacity. The result is then divided by the stress resulting from the live load (LL) stress including the necessary impact factor.

Fig. 12 shows the comparison of the load rating factors for each individual girder for both inventory and operating level stresses. Chen and Duan (2003) describe that the inventory rating is for vehicle loads frequently carried by the bridge and the operational rating is for less frequent heavier vehicles which allows the rating to be higher. It is noted that in Fig. 12 the load rating calculated with Virtis using NDT Data for girders two, three, and five are more than the conventional load rating. However, load ratings of girders one, four, and six, are the same because the stresses experienced by these beams during the load test were not large enough to increase the ratings according to AASHTO. Future truck load testing will include positioning heavier test trucks on load paths to get the largest response in each beam to increase the NDT rating for all girders.

The ratings using the calibrated FEM are generally more for each girder because this method benefits from calibration by the NDT data and fully captures the 3D behavior through the use of the baseline model. In this approach, an HS25 design truck was positioned to get the largest response for each girder. Six load paths were created by placing the left tire of the HS25 design truck directly on girder one and then the right wheel was placed on girders two through six. These six load paths were used in SAP2000 as moving truck loads to determine the critical strain locations and magnitudes. The resulting load rating factors for the calibrated-FEM are shown in Fig. 12. It should be noted that the rating factors for girders one to six are not symmetric because the bridge is not symmetric, since the sidewalk is on the east side of the bridge over girder six. The overall higher load rating factors represent the additional reserved load carrying capacity of the bridge. However, the load rating factors of the exterior girders in Fig. 12 are slightly lower than the first two methods because the steel railings and the sidewalk were not modeled in the FEM. This approach will lead to a more conservative load rating factors.

The baseline FEM predicted load rating factors for inventory and operating levels that were on average about double those calculated by using Virtis for the interior girders. These graphs show an increased rating factor using the calibrated baseline FEM. Although use of 3D system analysis and measured data may show additional capacity, bridge engineers should rely on engineering judgment and AASHTO/state guidelines to determine how much of an increase, if any, should be considered.

The ultimate benefit of the approach described by this article is the development of an improved understanding of the difference between expected bridge behavior and actual bridge performance. This is achieved through harnessing the FEM calibrated with respect to the measured bridge responses. Evaluating bridge performance by comparing the measured response to a maintained baseline model can provide a new objective understanding of long-term bridge behavior. It can provide valuable data to supplement regular bridge inspection and rating procedures. The data can help provide a basis for better decision making and use of limited resources for bridge maintenance. The need for advancement of technology in the field of SHM will increasingly support a long-term view for bridge monitoring and maintenance. Also, trends to date support that technology will advance to improve resilience and resistance to harsh conditions.

Conclusions

Bridge instrumentation for the purposes of static truck load testing was successfully installed during the construction phase without interfering with the construction process. Detailed 3D finite element modeling of typical highway bridges was shown to be feasible with a high degree of accuracy. Nondestructive testing performed on a newly constructed bridge provided highly reliable strain data to be used for calibrating a baseline FEM. The calibrated baseline model can be used for future SHM. Three types of load ratings were performed. First, the conventional load rating factors were determined according to AASHTO-specified analysis by using Virtis. Second, the load rating factors were updated by using NDT data, with the load test truck positions. The updated Virtis load rating factors using NDT data were overall more than conventional load rating factors attributable to the use of measured strains. Third, the FEM was calibrated by using the NDT data and was then used for load rating. Because the FEM benefits from the actual strain measurements and captures the 3D system behavior, it resulted in a higher overall load rating factor than the other two methods. Once resilience of sensors and technological advancements have matured, an updated FEM and monitoring system could be submitted to the bridge owner as part of the final design submission

J. Bridge Eng. 2012.17:130-138.

Downloaded from ascelibrary.org by Tufts University on 06/08/15. Copyright ASCE. For personal use only; all rights reserved.

to be used as a tool for SHM to assist in planning, bridge inspections, routine maintenance decisions, bridge load rating, damage assessment, and rehabilitation throughout the life of the bridge.

Acknowledgments

The writers are grateful for the funding of this research by NSF-PFI Grant No. 0650258. Any opinions, findings, and conclusions or recommendations expressed in this material are those of the authors and do not necessarily reflect the views of the National Science Foundation. Additionally, they would like to thank MassDOT and the Town of Barre for access to the Vernon Avenue Bridge, Fay Spofford & Thorndike Inc. for providing access to the design calculations and drawings, bridge constructor E.T. & L. Corporation and their subconsultants High Steel Structures Inc. and Atlantic Bridge and Engineering Inc. for their support and access during construction for instrumentation including accommodating researchers during instrumentation at the steel yard. Thanks to Geocomp Corporation for extensive help during the instrumentation phase. Additional thanks to graduate student Ms. Merve Iplikcioglu for making improvements to the load rating section.

References

Alampalli, S., and Lund, R. (2006). "Estimating fatigue life of bridge components using measured strains." *J. Bridge Eng.*, 11(6), 725–736.

American Association of State Highway and Transportation Officials. (2002). "Standard specifications for highway bridges, 17th ed." Washington, DC.

American Association of State Highway and Transportation Officials. (2010a). "Manual for bridge evaluation, 1st ed., with 2010 interims." C3, Washington, DC.

American Association of State Highway and Transportation Officials. (2010b). "AASHTO LRFD bridge design specifications, 5th ed." C4, Washington, DC.

Barr, P. J., Woodward, C. B., Najera, B., and Amin, Md N. (2006). "Long-term structural health monitoring of the San Ysidro Bridge." *J. Perform. Constr. Facil.*, 20(1), 14.

Cardini, A. J., and DeWolf, J. T. (2008). "Long-term structural health monitoring of a multi-girder steel composite bridge using strain data." *Struct. Health Monit.*, 8(1), 47–58.

Chen, Wai-Fah and Duan, Lian, eds. (2003). "Section 5.5—Fundamentals of bridge rating." *Bridge engineering: Construction and maintenance*, CRC Press, Boca Raton, FL.

Chajes, M. J., and Shenton, H. W., III (2005). "Using diagnostic load tests for accurate load rating of typical bridges." *Proc., 2005 Structures Congress and the 2005 Forensic Eng. Symp.*, Vol. 171, ASCE, Reston, VA, 2.

Chung, W., and Sotelino, E. D. (2006). "Three-dimensional finite element modeling of composite girder bridges." *Eng. Struct.*, 28(1), 63–71.

Computers and Structures Inc. (2000). "Integrated finite element analysis and design of structures." SAP 2000, Berkeley, CA.

Doebling, S., Farrar, C., Prime, M., and Shevits, D. (1996). "Damage identification and health monitoring of structural and mechanical systems from changes in their vibration characteristics: A literature review." *Los Alamos National Laboratory Rep. No. LA-13070-MA*, Los Alamos, NM.

Federal Highway Administration. (2009). "Traffic volume trends." ⟨www.fhwa.dot.org⟩.

Jauregui, D. V., and Barr, P. J. (2004). "Nondestructive evaluation of the I-40 bridge over the Rio Grande River." *J. Perform. Constr. Facil.*, 18(4), 195–204.

Thomas Kuesel, R. (1990). "Whatever happened to long-term bridge design?" *Civil Eng.*, 6(2), 57–60.

Mabsout, M. E., Tarhini, K. M., Frederick, G. R., and Tayar, C. (1997). "Finite-element analysis of steel girder highway bridges." *J. Bridge Eng.*, 2(3), 83–87.

MA Highway Department. (2005). "Bridge manual, Part I and Part II, 2005 ed."

Phelps, J. E. (2010). "Instrumentation, non destructive testing, and finite element model updating for bridge evaluation." M.S. thesis, Tufts Univ., Medford/Somerville, MA.

Sanayei, M., Imbaro, R. G., McClain, A. S. J., and Brown, C. L. (1997). "Structural model updating using experimental static measurements." *J. Struct. Eng.*, 123(6), 792.

Sanayei, M., and Onipede, O. (1991). "Damage assessment of structures using static test data." *AIAA J.*, 29(7), 1174–1179.

Sanayei, M., Onipede, O., and Babu, S. R. (1992). "Selection of noisy measurement locations for error reduction in static parameter identification." *AIAA J.*, 30(9), 2299–2309.

Sanayei, M., and Saletnik, M. J. (1996). "Parameter estimation of structures from static strain measurements. I: Formulation." *J. Struct. Eng.*, 122(5), 555–562.

Schlune, H., Plos, M., and Gylltoft, K. (2009). "Improved bridge evaluation through finite element model updating using static and dynamic measurements." *Eng. Struct.*, 31(7), 1477–1485.

Sohn, H., Farrar, C. R., Hemez, F. M., Shunk, D. D., Stinemates, D. W., and Nadler, B. R. (2003). "A review of structural health monitoring literature: 1996–2001." *Los Alamos National Laboratory Rep., LA-13976-MS*.

Stanton et al. (2008). "Rotation limits for elastomeric bearings." *National Cooperative Highway Research Program-Rep. 596*, Transportation Research Board.

Yost, J. R., Schulz, J. L., and Commander, B. C. (2005). "Using NDT data for finite element model calibration and load rating of bridges." *Metropolis and Beyond Proc. of the 2005 Structures Congress and the 2005 Forensic Eng. Symp.*, New York, 171, 3.

Zhang, Z., and Aktan, A. E. (1997). "Different levels of modeling for the purpose of bridge evaluation." *Appl. Acoust.*, 50(3), 189–204.

Downloaded from ascelibrary.org by Tufts University on 06/08/15. Copyright ASCE. For personal use only; all rights reserved.